

## SUPPORTING INFORMATION

### Flow Synthesis of Iron Oxide Nanoparticles: Using Multiple Precursor Additions to Improve Size Control

Agus R. Poerwoprajitno,<sup>a</sup> Alexander Malaj,<sup>b</sup> O. Thompson Mefford,<sup>b</sup> Dale L. Huber,<sup>a\*</sup>

<sup>a</sup> Center for Integrated Nanotechnologies, Sandia National Laboratories, Albuquerque, NM 87185 (USA)

<sup>b</sup> Department of Materials Science & Engineering, Clemson University, Clemson, SC 29634 (USA)

#### Experimental details

**Synthesis of iron oxide nanoparticles (batch method).** The synthesis of iron oxide nanoparticles was adapted from ref [1]. Iron(III) acetylacetonate (1 mmol, Aldrich, 97%), oleylamine (5 mL, Aldrich, 98%), and benzyl ether (5 mL, Aldrich, 98%) were mixed in a 100 mL three-necked round-bottom flask. The mixture was heated to 110 °C molten metal bath containing Bolton 174, a low-melting-point Bi-Sn-In alloy (Bolton Metal Products, Bellefonte, PA), under a nitrogen flow for 1 h to remove residual moisture. The reaction was then rapidly heated to 250 °C and maintained at this temperature for 1 h. After cooling to room temperature, the nanoparticles were purified by precipitation using a hexane/acetone mixture, followed by centrifugation at 13,000 rpm for 30 min.

**Synthesis of iron oxide nanoparticles in microfluidics.** For microfluidic synthesis, iron(III) acetylacetonate (1 mmol, Aldrich, 97%) was dissolved in benzyl ether (5 mL, Aldrich, 98%) and oleylamine (5 mL, Aldrich, 98%). The solution was first heated in a 110 °C molten metal bath (Bolton 174 alloy) under nitrogen for 1 h to remove moisture, then cooled to room temperature before injection into the microfluidic device. The chip was maintained at 250 °C using a custom-built heater (Figure S1) and enclosed in a nitrogen-filled zip bag. A 100 mM precursor solution was injected at a flow rate of 1.5 mL h<sup>-1</sup> using a syringe pump, and the product was collected in centrifuge tubes. For experiments requiring additional precursor, the iron concentration was adjusted by adding equivalent amounts of benzyl ether and oleylamine. After each synthesis, the microfluidic chip was cleaned by flushing with hexane at 100 µL min<sup>-1</sup> followed by 0.1M HCl solution to prevent clogging. The nanoparticles were purified by precipitation with hexane/acetone and centrifugation at 13,000 rpm for 30 min. The reaction mixture was collected at different locations on the chip (see page 8-9) and the supernatant analyzed by UV-Vis spectroscopy and converted to a concentration using a calibration curve generated from Fe(acac)<sub>3</sub> standards prepared in an identical solvent and stabilizing agent matrix.

**Characterization.**

X-ray diffraction (XRD) samples were prepared by drop-casting several drops of concentrated nanoparticle suspension onto a silicon substrate, followed by solvent evaporation. XRD patterns were collected on a Rigaku SmartLab diffractometer equipped with a Cu K $\alpha$  radiation source (40 kV, 44 mA). Phase identification was performed using Rigaku PDXL analytical software in combination with the ICDD PDF-2 database (release 2010 RDB).

Transmission electron microscopy (TEM) samples were prepared by drop-casting a dispersion of nanoparticles in hexane onto carbon-coated copper grids. Initial screening was carried out using an FEI Tecnai microscope, and high-resolution TEM images (Figure 1) were obtained on an FEI Titan ETEM equipped with an image Cs corrector and operated at 300 kV. Particle size distributions were determined from at least 100 nanoparticles using ImageJ software.

**Magnetic measurements.**

DC magnetization curves were recorded at 298 K over a field range of  $-2.38 \times 10^3$  to  $+2.38 \times 10^3$  kA m $^{-1}$  using a Quantum Design VersaLab vibrating sample magnetometer (VSM). The measured magnetic moment was normalized to the mass of magnetite. To determine this mass, nanoparticles were digested in 4.5 mL HCl and analyzed by inductively coupled plasma-optical emission spectroscopy (ICP-OES). ICP-OES was used to determine the Fe content of the VSM sample which was converted to a mass of Fe $_3$ O $_4$ . The magnetic moment reported in Figure S10 is normalized based on the mass of Fe $_3$ O $_4$ .

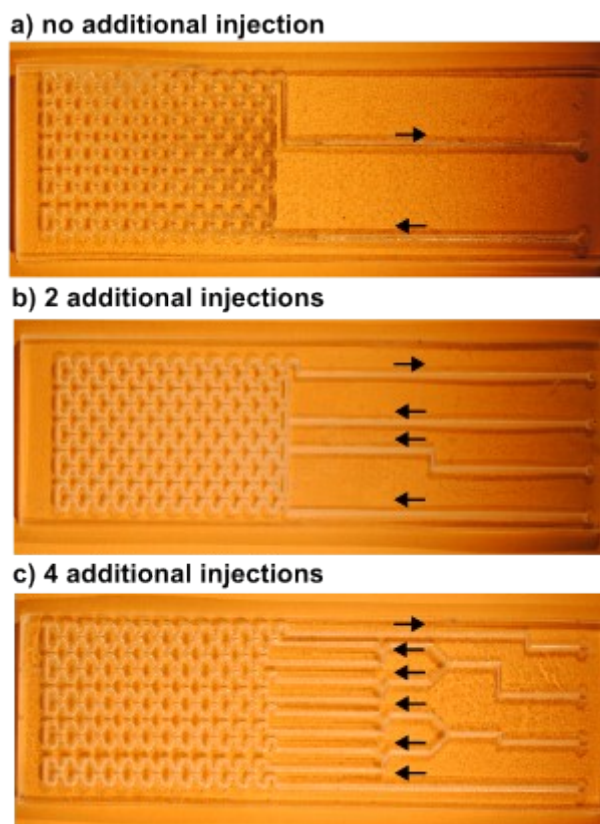


**Figure S1.** Photos of microfluidic chips with a) no additional injection, b) two additional injections, and c) four additional injections. Arrows indicate the direction of flow. Each microfluidic chip measures  $3 \times 1$  inches. The serpentine portions of the chip were inserted into a thermostatted aluminum heating block to induce the thermal decomposition.

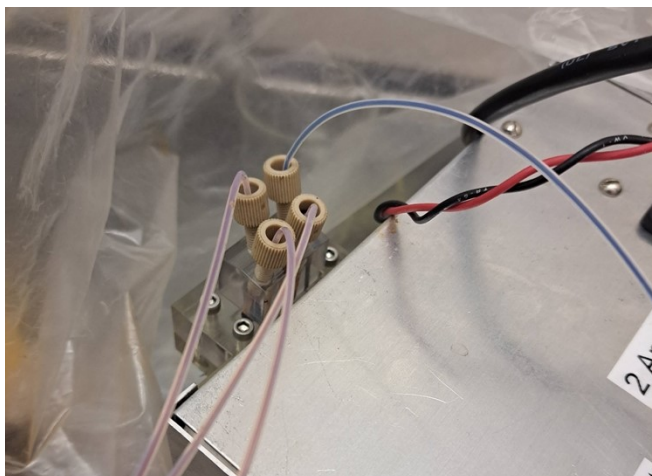


**Figure S2.** Photo of the input flow containing Fe precursor (red color solution) and the output flow containing the resulted iron oxide nanoparticles (black color solution).

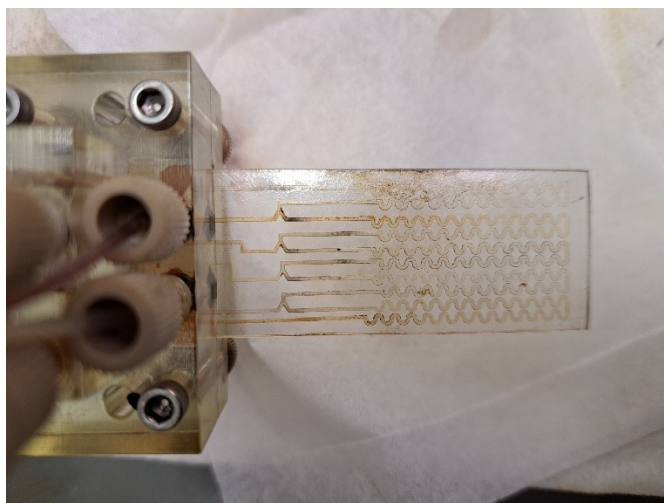


**Figure S3.** Photo of the microfluidic chip after reaction and cleaning.

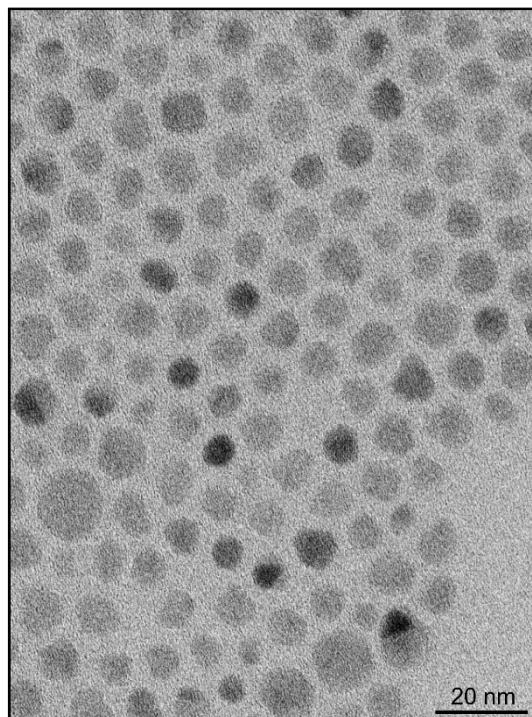


**Figure S4.** TEM image of synthesized iron oxide nanoparticles by microfluidic without additional injection.

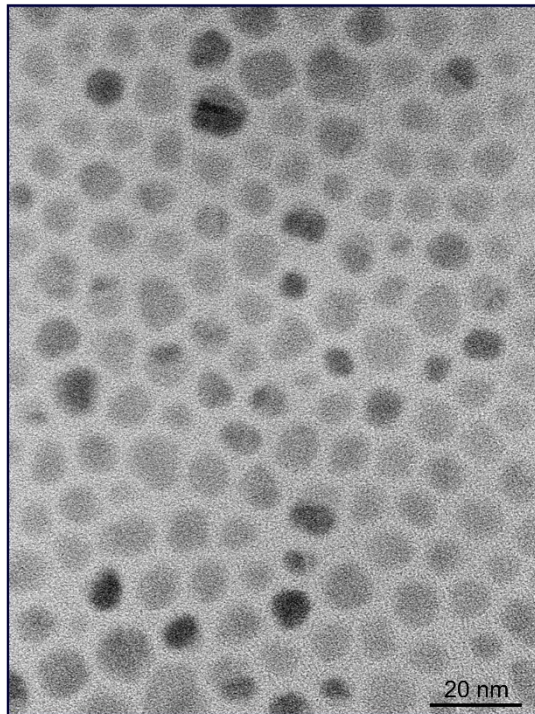


**Figure S5.** TEM image of synthesized iron oxide nanoparticles by microfluidic with 2 additional injections.

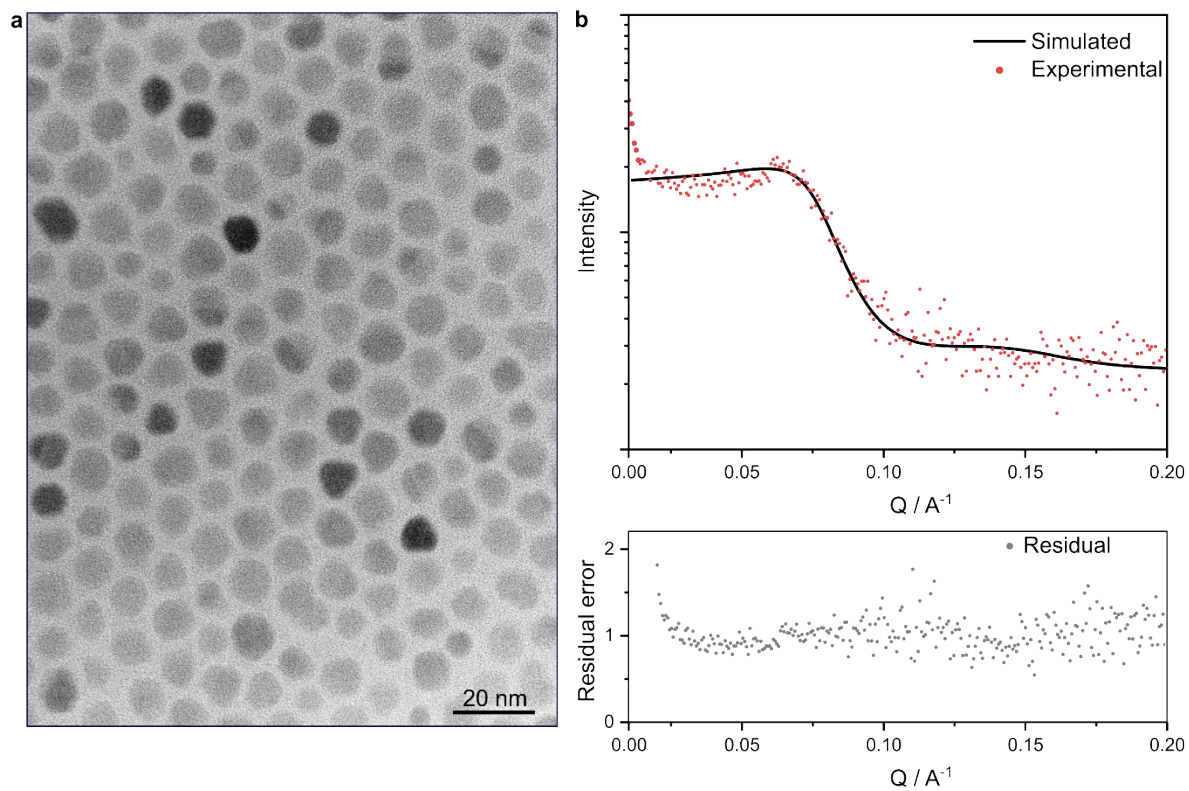


**Figure S6. a)** TEM image and **(b)** SAXS pattern of synthesized iron oxide nanoparticles by microfluidic with 4 additional injections.

## UV-Vis experiment

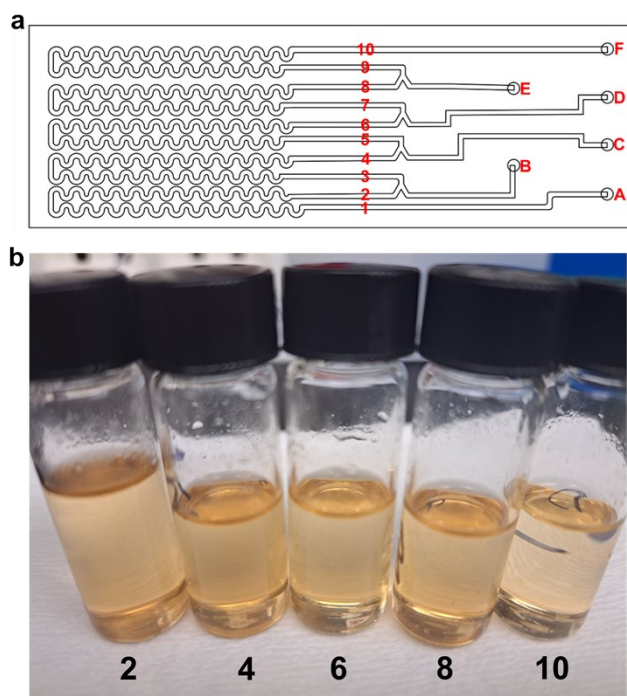


**Figure S7.** a) A scheme of the microfluidic chip with 4 additional injections. The numbers show where the data points are collected for UV-Vis analysis. b) Photos of the aliquots.

To elucidate the Extended LaMer mechanism, the concentration of iron precursor was analyzed by UV-Vis from 10 different locations.

- The first data point was taken from point A which is the concentration of iron precursor before reaction.
- Firstly, we did not inject any additional precursor. Therefore, the solution will go to point B as the second data point.
- We then injected solution from point B with a concentration of 33 mM at a injection rate of  $2.5 \mu\text{l min}^{-1}$ . This solution will mix with the solution no.2 that has concentration of 4 mM to give mixed concentration of 13.7 mM with a flow rate of  $7.5 \mu\text{l min}^{-1}$ .
- We then repeated this procedure to give total of 10 data points.

**Table S1.** Concentration of iron precursor in microfluidic chip over time with 4 additional precursor injections.

	[Fe] (mM)	Flow rate ( $\mu\text{l min}^{-1}$ )	Time (s)
1	100	5	0
2	4	5	300
3	13.7	7.5	300
4	8	7.5	540
5	14.3	10	540
6	7.5	10	740
7	12.6	12.5	740
8	8.6	12.5	911
9	12.7	15	911
10	8.4	15	1061

The rate of reaction can be described using the following equation:

$$\text{Rate of reaction} = -\Delta [\text{Fe}] / \Delta t = k [\text{Fe}]^x$$

**Table S2.** Rate of reaction of the consumption of iron precursor in the microfluidic chip

Initial [Fe]	Rate (mM/s)
100	0.32
13	0.023
14	0.033
12	0.023
13	0.028

From table S2, it can be calculated that the reaction follows first-order reaction with the rate being simplified as:

$$\text{Rate of reaction} = k [\text{Fe}]$$

where k is  $2.8 \cdot 10^{-3} \text{ s}^{-1}$

### Calculation of yield:

$$\text{Reacted Fe precursor} = (\text{Flow rate} \times \text{concentration})_{\text{input}} - (\text{Flow rate} \times \text{concentration})_{\text{output}}$$

$$\text{Reacted Fe precursor} = (5 \mu\text{l}/\text{min} \times 100 \text{ mM}) + (5 \times 2.5 \mu\text{l}/\text{min} \times 33 \text{ mM}) - (17.5 \mu\text{l}/\text{min} \times 8.4 \text{ mM})$$

$$\text{Reacted Fe precursor} = 765.5 \times 10^{-6} \text{ mmol}/\text{min}$$

$$\text{Reacted Fe precursor} = 1.1 \text{ mmol}/\text{day}$$

$$\text{Synthesized magnetite} = 85 \text{ mg}/\text{day}$$

### Calculation of Reynolds number

- Circular channel/tube diameter  $D = 5 \times 10^{-4} \text{ m}$
- Density  $\rho = 920 \text{ kg}/\text{m}^3$
- Dynamic viscosity  $\mu = 0.63 \text{ cp} = 0.63 \times 10^{-3} \text{ Pa s}$  (log-mixing rule)
- Volumetric flow  $Q = 1.5 \text{ ml}/\text{hr} = 4.2 \times 10^{-10} \text{ m}^3/\text{s}$

$$Re = \frac{\rho V D}{\mu} = 1.53$$

**Table S3.** Reproducibility of iron oxide nanoparticle synthesis at different numbers of additional injections.

Additional injections	Run	Size (nm)	CV (%)
0	I	7.0	21.3
	II	7.4	21.6
	III	7.2	19.2
2	I	7.3	13.1
	II	6.8	17.7
	III	7.0	16.5
4	I	8.0	9.8
	II	8.4	11.9
	III	8.2	10.5

**Table S4.** Comparison of coefficient of variation (CV) to the literature.

Reference	CV (%)
This work	9.8-11.9
<i>Chem. Mater.</i> , 2015, <b>27</b> , 1299-1305	14.3
<i>Particuology</i> , 2016, <b>26</b> , 47-53	33.5
<i>Chemical Engineering Journal</i> , 2018, <b>340</b> , 66-72	21.0
<i>Chemical Engineering Journal</i> , 2023, <b>473</b> , 144542	13.6
<i>Lab on a Chip</i> , 2023, <b>23</b> , 115-124	21.3

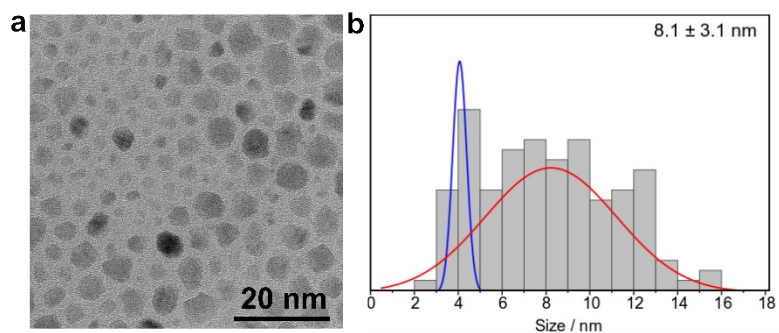


**Figure S8.** TEM image (a) and statistical analysis (b) of the iron oxide nanoparticles synthesized by 70 mM Fe precursor.

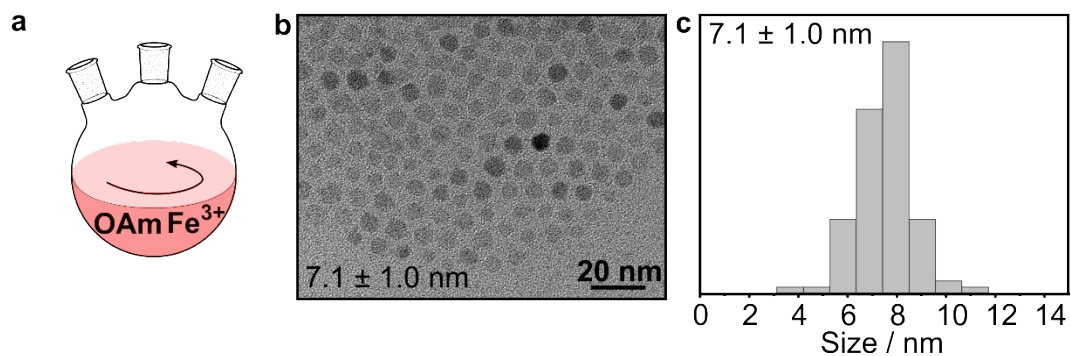


**Figure S9.** a) a schematic illustration of the bench top process. b-c) TEM image, size distribution of iron oxide nanoparticles synthesized by a bench top reaction.

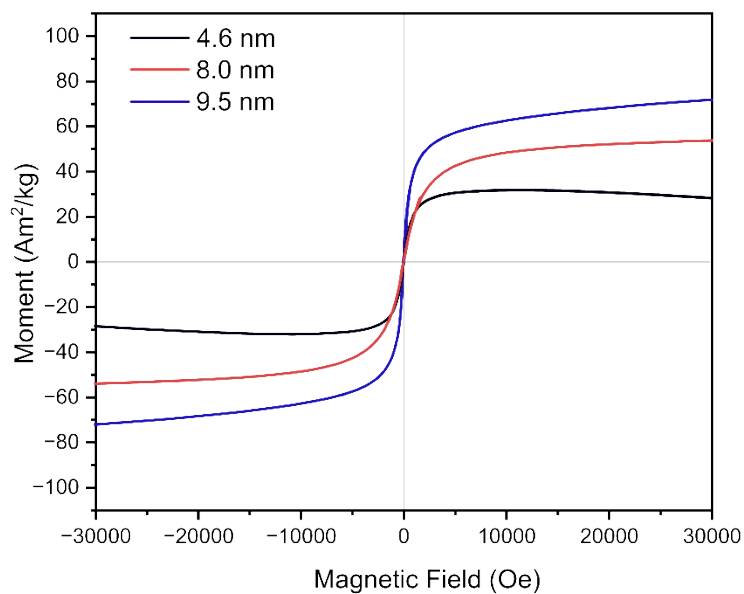


**Figure S10.** Magnetization versus applied magnetic field for the nanoparticles of 4.6 nm (black), 8.0 nm (red) and 9.5 nm (blue) Fe<sub>3</sub>O<sub>4</sub> nanoparticles at 300 K.

**References:**

- [1] Z. Xu, C. Shen, Y. Hou, H. Gao and S. Sun, *Chem. Mater.*, 2009, **21**, 1778-1780.